

MOL #56978

## TITLE PAGE

### **Cyclin-Dependent Kinase 5 Inhibitors: Inhibition of Dopamine Transporter Activity**

David A. Price, Alexander Sorkin and Nancy R. Zahniser

*Department of Pharmacology (D.A.P., A.S., N.R.Z.); Neuroscience Program (A.S., N.R.Z.),  
University of Colorado Denver, Aurora, CO*

MOL #56978

## RUNNING TITLE PAGE

**Running Title:** Cdk5 inhibitors reduce DAT activity

**Corresponding Author:**

Dr. David A. Price  
University of Colorado Denver  
Department of Pharmacology  
Mail Stop 8303, RC1-North Tower, P18-6402K  
12800 East 19<sup>th</sup> Avenue  
Aurora, CO 80045  
Office: (303) 724-3657  
Fax: (303) 724-3663  
E-mail: [David.A.Price@ucdenver.edu](mailto:David.A.Price@ucdenver.edu)

**Number of Text Pages:** 39

**Number of Tables:** 0

**Number of Figures:** 8

**Number of References:** 40

**Number of Words in the Abstract:** 244

**Number of Words in the Introduction:** 715

**Number of Words in the Discussion:** 1372

**Abbreviations:** Cdk5, cyclin-dependent kinase 5; DA, dopamine; DAT, dopamine transporter; dSTR, dorsal striatal/striatum; hDAT; human dopamine transporter; AMPH, amphetamine; PKA, cAMP-dependent protein kinase A; PKC, protein kinase C; PI3K, phosphatidylinositol 3-kinase; MAPK, p44/42 mitogen-activated protein kinase; CaMKII, Ca<sup>2+</sup>/calmodulin-dependent protein kinase II; Ser, serine; Thr, threonine; DARPP-32, DA and cAMP-regulated phospho-protein of relative molecular mass 32,000; TH, tyrosine hydroxylase; PAE, porcine aortic endothelial; YFP, yellow fluorescent protein; HA, hemagglutinin epitope; PMA, 12-myristate 13-acetate; DMSO, dimethyl sulfoxide; PP2A-A  $\alpha/\beta$ , protein phosphatase 2A-A  $\alpha/\beta$ ; Cy5 or Cy3, cyanine 5 or 3, respectively; NT-siRNA, Dharmacon siGENOME non-targeting #3 siRNA; BSA, bovine serum albumin; CMF-PBS, Ca<sup>2+</sup>/Mg<sup>2+</sup>-free phosphate buffered saline; TBS-T, 0.1% Tween 20/Tris-buffered saline; IC<sub>50</sub>, half-maximal inhibition; V<sub>max</sub>, maximal uptake velocity; K<sub>m</sub>, substrate affinity; ANOVA, analysis of variance

MOL #56978

## ABSTRACT

Cyclin-dependent kinase 5 (Cdk5) reduces the rewarding properties of psychostimulants by dampening postsynaptic dopamine (DA) receptor signaling. Cdk5 is also present in midbrain DA neurons, where the DA transporter (DAT) is localized and limits DA neurotransmission by removing extracellular DA. Here, we tested the hypothesis that Cdk5 could also impact the disposition of DA by regulating DAT activity. Incubation of rat dorsal striatal (dSTR) synaptosomes with the Cdk5 inhibitors roscovitine, olomoucine, GW8510 or the inactive congener *iso*-olomoucine, resulted in a rapid, concentration-dependent inhibition of specific [ $^3$ H]DA uptake. However, roscovitine was the only inhibitor that did not also decrease [ $^3$ H]WIN35,428 binding to dSTR DATs. Roscovitine-induced inhibition of dSTR [ $^3$ H]DA uptake was explained by decreased maximal uptake velocity, without a change in cell-surface DAT levels. Roscovitine did not enhance [ $^3$ H]DA release mediated by either DAT reverse-transport or  $\text{Ca}^{2+}$  channels in dSTR slices. Instead, roscovitine enhanced spontaneous [ $^3$ H]DA outflow and inhibited DAT-mediated [ $^3$ H]DA re-accumulation into dSTR slices. To explore the involvement of Cdk5 in roscovitine-induced down-regulation of DAT activity, Cdk5 protein was knocked-down via Cdk5-siRNA by as much as 86% in porcine aortic endothelial cells stably expressing human (h)DATs. However, Cdk5 depletion did not alter hDAT activity. Taken together, our results suggest that roscovitine inhibits DAT activity independently of Cdk5 and, therefore, results obtained with such inhibitors should be interpreted with caution. Our study is the first to demonstrate that Cdk5 inhibitors reduce brain DAT activity via a mechanism that is independent of DAT trafficking and reverse-transport.

MOL #56978

## INTRODUCTION

Dopamine (DA) neurotransmission and its related neural functions underlie psychomotor control, affect and rewarding behaviors (Schultz, 2007). Importantly, dysfunctional DA neurotransmission contributes, in part, to the clinical manifestations of Parkinson's disease, schizophrenia and drug addiction. The DA transporter (DAT) is a plasmalemmal membrane carrier protein that contributes to spatial-temporal regulation of DA signaling. This is accomplished by the active removal of extracellular DA through functional DAT molecules, which are located on the cell-surface of DA neuronal axons, varicosities and dendrites (Nirenberg et al., 1996). In addition to helping maintain DA homeostasis, the DAT is a molecular target of psychostimulants such as cocaine and amphetamine (AMPH) (Giros et al., 1996; Chen et al., 2006).

Significant progress during the last decade has demonstrated that DATs are rapidly regulated via trafficking-dependent and -independent mechanisms (Blakely and Bauman, 2000; Zahniser and Sorkin, 2009). In addition to DAT regulation by psychostimulants, several protein kinases influence DAT activity. These include: cAMP-dependent protein kinase A (PKA) (Pristupa et al., 1998); protein kinase C (PKC) (Daniels and Amara, 1999; Melikian and Buckley, 1999; Chen et al., 2009); phosphatidylinositol 3-kinase (PI3K) (Carvelli et al., 2002); p44/42 mitogen-activated protein kinase (MAPK) (Moron et al., 2003); Akt (Garcia et al., 2005); Ca<sup>2+</sup>/calmodulin-dependent protein kinase II (CaMKII) (Fog et al., 2006); and protein tyrosine kinases (Hoover et al., 2007). Although many protein kinases and their inhibitors alter DAT activity by changing the number of functional cell-surface DATs, DAT phosphorylation by protein kinases can also alter DAT activity independent of changes in trafficking (Foster et al., 2006).

MOL #56978

Cyclin-dependent kinase 5 (Cdk5) is a serine/threonine (Ser/Thr) protein kinase that is ubiquitously expressed in the adult rat brain (Zheng et al., 1998). Cdk5 plays important roles in several neural processes, ranging from neurodevelopment and migration to synaptic transmission and plasticity (Dhavan and Tsai, 2001). The identification of DA and cAMP-regulated phosphoprotein of relative molecular mass 32,000 (DARPP-32) as a substrate of Cdk5 provided the first evidence that Cdk5 also impacts DA neurotransmission (Bibb et al., 1999). Phosphorylation of DARPP-32 by Cdk5 diminishes postsynaptic DA receptor-mediated signaling (Bibb et al., 2001). Subsequently, it was shown that: 1) repeated exposure to cocaine elevates Cdk5 expression in both dorsal striatum (dSTR) and nucleus accumbens (Bibb et al., 2001) and 2) pharmacological inhibition (Bibb et al., 2001; Taylor et al., 2007) or knockdown (Benavides et al., 2007) of Cdk5 augments cocaine-induced behavioral activation/sensitization and incentive-motivational processes. Thus, Cdk5 appears to be a compensatory negative regulator of postsynaptic DA signaling following psychostimulant exposure.

In addition to the convincing evidence for a role of Cdk5 in regulating postsynaptic DA signaling events, several studies indicate that Cdk5 may also modulate DA neurotransmission by acting presynaptically within DA neurons. Importantly, Cdk5 mRNA is expressed in DA-containing brain regions such as the substantia nigra pars compacta (Chergui et al., 2004) where Cdk5 protein co-localizes in cells immunoreactive for the rate-limiting enzyme of DA synthesis, tyrosine hydroxylase (TH) (Smith et al., 2003). Additional evidence for a role of Cdk5 within DA neurons is supported by findings that: 1) Cdk5 inhibitors potentiate evoked DA release from striatal slices (Chergui et al., 2004) and 2) Cdk5 phosphorylates TH, thereby enhancing its stability (Kansy et al., 2004; Moy and Tsai, 2004).

MOL #56978

Here, we tested the hypothesis that Cdk5 may also rapidly regulate brain DAT activity, which would represent another presynaptic mechanism whereby Cdk5 could impact DA neurotransmission. We used rat dSTR synaptosomes and slices containing dSTR to measure the effects of several Cdk5 inhibitors on: 1) specific [ $^3\text{H}$ ]DA uptake, 2) cell-surface DAT levels and 3) [ $^3\text{H}$ ]DA efflux/release. Cdk5 inhibitors used here included: the widely used inhibitor roscovitine and the less selective inhibitor olomoucine (Meijer et al., 1997); *iso*-olomoucine, an inactive congener of olomoucine (Vesely et al., 1994); and the structurally dissimilar inhibitor GW8510, which displays selectivity towards Cdk5 in neuronal tissues (Johnson et al., 2005). Porcine aortic endothelial (PAE) cells stably expressing yellow fluorescent protein (YFP)-hemagglutinin epitope (HA)-human (h)DATs (Sorkina et al., 2006) were used to explore further the findings from rat brain tissue and to test, by using Cdk5-siRNA, the involvement of Cdk5 in the pharmacological effects of roscovitine. Our findings demonstrate, for the first time, that Cdk5 inhibitors rapidly down-regulate DAT activity via a mechanism(s) that is independent of DAT trafficking and reverse-transport and, most likely, occurs in a Cdk5-independent manner.

MOL #56978

## MATERIALS AND METHODS

**Materials.** Unless stated otherwise, laboratory chemicals were purchased from Fisher Scientific (Pittsburgh, PA) or Sigma (St. Louis, MO). Roscovitine InSolution™, olomoucine InSolution™ and *iso*-olomoucine were purchased from Calbiochem (San Diego, CA). (–)-cocaine HCl was a generous gift from the National Institute on Drug Abuse (Research Triangle International; Research Triangle Park, NC). DA hydrochloride (DA), GW8510, benztropine methane sulfonate, d-AMPH sulfate salt (AMPH) and 12-myristate 13-acetate (PMA) were purchased from Sigma. Cdk5 inhibitors and PMA were dissolved in dimethylsulfoxide (DMSO) and diluted to a final assay concentration of 0.1% DMSO, unless stated otherwise. All other drugs were diluted in assay buffer. [<sup>3</sup>H]DA (specific activity = 40.0-55.0 Ci/mmol), [<sup>3</sup>H]alanine (specific activity = 85 Ci/mmol), [<sup>3</sup>H]leucine (specific activity = 115.4 Ci/mmol) and [<sup>3</sup>H]WIN35,428 (specific activity = 86.0 Ci/mmol) were purchased from Perkin-Elmer Life Sciences (Boston, MA). Sulfo-NHS-biotin, monomeric avidin beads and enhanced chemiluminescent substrate were obtained from Pierce Chemical (Rockford, IL). The mouse monoclonal DAT antibody was a generous gift from Dr. Roxanne Vaughan (University of North Dakota; Grand Forks, ND). Other antibodies were purchased from the following sources: rabbit monoclonal phospho-MAPK (Thr202/Tyrosine 204), polyclonal rabbit MAPK, rabbit polyclonal Cdk5 and goat anti-rabbit IgG HRP secondary antibody from Cell Signaling Technology (Beverly, MA); mouse monoclonal protein phosphatase 2A-A  $\alpha/\beta$  (PP2A-A  $\alpha/\beta$ ) from Santa Cruz Biotechnology (Santa Cruz, CA); goat anti-mouse IgG HRP secondary antibody from BioRad (Hercules, CA); mouse monoclonal HA11 from Covance (Berkley, CA); and donkey anti-mouse secondary antibody conjugated with cyanine 5 (Cy5) or 3 (Cy3) from Jackson ImmunoResearch (West Grove, PA).

MOL #56978

**Animals.** Male Sprague-Dawley rats (150-200 g, 6-8 week old; Charles River Laboratories; Wilmington, MA) were group-housed (n = 4 rats per cage) on a 12-hr light/dark cycle with *ad libitum* access to food and water. All procedures involving the use of animals were carried out in accordance with the NIH *Guide for the Care and Use of Laboratory Animals* and were approved by the Institutional Animal Care and Use Committee of the University of Colorado Denver.

**Cell culture and transfections.** PAE cells stably expressing YFP-HA-hDAT were grown in Ham's F-12 medium containing 10% fetal bovine serum (Invitrogen; Eugene, OR) as previously described (Sorkina et al., 2006). DharmaFECT I transfection reagent, siGENOME non-targeting #3 siRNA (NT-siRNA) and siGENOME SMARTpool Cdk5-siRNA were purchased from Dharmacon (Chicago, IL). Cells were transfected according to the manufacturer's recommendations and were processed for individual experiments seventy-two hours post-transfection. The final concentration of non-targeting siRNA for all assays was 100 nM.

**Preparation of rat dSTR synaptosomes.** dSTR synaptosomes were prepared as previously described in detail (Hoover et al., 2007).

**Synaptosomal [<sup>3</sup>H]ligand uptake.** Specific uptake of [<sup>3</sup>H]ligand into dSTR synaptosomes was measured as previously described (Hoover et al., 2007). P2 synaptosomes, resuspended in ice-cold sodium phosphate assay buffer (in mM: 134 NaCl, 4.8 KCl, 1.3 CaCl<sub>2</sub>, 1.4 MgSO<sub>4</sub>, 3.3 NaH<sub>2</sub>PO<sub>4</sub>•H<sub>2</sub>O, 12.7 Na<sub>2</sub>HPO<sub>4</sub>, 11 glucose, 1 ascorbic acid; pH 7.4), were incubated with drug for the indicated time at 37°C with gentle shaking. For studies in which inhibitor was washed out, synaptosomes were incubated with or without roscovitine for 30 min at 37°C with shaking. Samples were then cooled on ice, centrifuged at 12,500 x g for 15 min at 4°C, resuspended in ice-cold assay buffer and re-centrifuged. The resulting P4 synaptosomes were resuspended in ice-cold assay buffer and then pre-incubated for 15 min at 37°C with gentle shaking. Uptake was



MOL #56978

initiated by the addition of [ $^3\text{H}$ ]DA (0.5 nM), [ $^3\text{H}$ ]alanine (10 nM) or [ $^3\text{H}$ ]leucine (10 nM) for 3 min at 37°C with gentle shaking. For kinetic analyses of [ $^3\text{H}$ ]DA/DA uptake, unlabelled DA was added concomitantly with 0.5 nM [ $^3\text{H}$ ]DA such that the final concentration of [ $^3\text{H}$ ]DA/DA was 0, 0.5, 5, 10, 50, 100, 200 or 500 nM. Non-specific uptake was determined either in the presence of cocaine (100  $\mu\text{M}$ ) for [ $^3\text{H}$ ]DA uptake or at 0°C for [ $^3\text{H}$ ]alanine and [ $^3\text{H}$ ]leucine uptake. At the end of uptake assays, samples were placed on ice and collected onto Whatman GF/B glass microfiber filters via rapid vacuum filtration using a tissue harvester (Brandel; Gaithersburg, MD). Filters were then washed three times with ice-cold 0.32 M sucrose buffer before being processed for scintillation counting. Protein content was measured via the method of Bradford (1976) using bovine serum albumin (BSA) as the standard.

**[ $^3\text{H}$ ]WIN35,428 binding.** Membrane binding assays were carried out according to published methods (Coffey and Reith, 1994). Rat dSTR was homogenized in ice-cold assay buffer (0.32 M sucrose, 30 mM  $\text{NaH}_2\text{PO}_4 \cdot \text{H}_2\text{O}$ , 15 mM  $\text{Na}_2\text{HPO}_4$ ; pH 7.4) with a Polytron (20-sec pulse; Brinkman; Westbury, NY). The homogenate was centrifuged at 20,000 x g for 20 min at 4°C, and the pellet was resuspended in assay buffer (15 mg/ml wet tissue weight) and dispersed with a Polytron (5-sec pulse). Binding of [ $^3\text{H}$ ]WIN35,428 (4 nM) was measured in the absence (total binding) or presence of drug. For studies measuring AMPH competition with [ $^3\text{H}$ ]WIN35,428 binding, vehicle or roscovitine was added concomitantly with AMPH and [ $^3\text{H}$ ]WIN35,428. Non-specific binding was measured in the presence of the DAT inhibitor benztropine (2.4  $\mu\text{M}$ ). Following incubation for 60 min at 4°C, binding was terminated by rapid vacuum filtration (see above) and three washes with 4°C sucrose-free assay buffer before processing for scintillation counting. Protein was measured by the method of Bradford (1976).

MOL #56978

**Cell-surface biotinylation.** Total and cell-surface (i.e. biotinylated) DAT levels from dSTR synaptosomes were measured as previously described in detail (Hoover et al., 2007).

**Immunoblotting.** Immunoblots were performed on drug-treated dSTR synaptosomes, biotinylated synaptosomal preparations (see above) and YFP-HA-hDAT-PAE cells. P2 dSTR synaptosomes, resuspended in sodium phosphate assay buffer (see above), were incubated with drug for 30 min at 37°C with gentle shaking. Samples were cooled on ice and centrifuged at 12,500 x g for 15 min at 4°C. The resulting synaptosomal pellet was resuspended in 90°C lysis buffer (1% SDS, 10 mM Trizma base, 10 mM EDTA; pH 7.4) and sonicated. PAE cells were washed three times with  $\text{Ca}^{2+}/\text{Mg}^{2+}$ -free phosphate buffered saline (CMF-PBS), and proteins were solubilized in Triton X-100/glycerol/HEPES lysis buffer as previously described (Sorkina et al., 2005). Protein content was measured using the BCA method (Pierce Chemical). Samples were placed in loading buffer (62.5 mM Trizma base; pH 6.8, 2% SDS, 10% glycerol, 5%  $\beta$ -mercaptoethanol, 8 mM DL-dithiothreitol, trace of bromophenol blue), heated for 5 min at 100°C and stored at -80°C until use. Proteins were separated by 7.5% (DAT and PP2A-A  $\alpha/\beta$  only) or 12% SDS-polyacrylamide gel electrophoresis before transferring to polyvinylidene difluoride membranes. Membranes were blocked in 5% non-fat dry milk in 0.1% Tween 20/Tris-buffered saline (TBS-T; 140 mM NaCl, 20 mM Trizma base; pH 7.6) for 60 min at 22-25°C. Membranes were then incubated overnight at 4°C with primary antibodies diluted in TBS-T containing BSA or block, as indicated: phospho-MAPK (1:2000 in 5% BSA), MAPK (1:1000 in 5% BSA), DAT (1:10,000 in 3% BSA), PP2A-A  $\alpha/\beta$  (1:5000 in block), Cdk5 (1:1000 in 5% BSA) or  $\beta$ -actin (1:1000 in 5% BSA). Membranes were then incubated with the appropriate horseradish peroxidase-conjugated secondary antibody for 60 min or 120 min (DAT

MOL #56978

immunoblots only) at 22-25°C before visualizing immunoreactive bands by enhanced chemiluminescence.

**[<sup>3</sup>H]DA release from rat dSTR slices.** Experiments measuring [<sup>3</sup>H]DA outflow (i.e. spontaneous release) and overflow (i.e. efflux/release above outflow) were performed according to published methods (Dwoskin and Zahniser, 1986). Briefly, following decapitation, 400 µm slices were cut with a vibratome and dSTR was dissected out. dSTR slices were incubated in Krebs' buffer saturated with 95% O<sub>2</sub>-5% CO<sub>2</sub> for 30 min at 35°C with gentle shaking. Slices were then loaded with [<sup>3</sup>H]DA (0.1 µM) by incubating for 30 min at 35°C with gentle shaking. Individual slices were transferred to glass chambers, maintained at 35°C, and superfused with Krebs' buffer saturated with 95% O<sub>2</sub>-5% CO<sub>2</sub> at a rate of 1 ml/min. Slices were allowed to stabilize for 75 min, when basal [<sup>3</sup>H]DA outflow was present at a low, constant level. Superfusate samples from individual slices were collected at 5-min intervals. Drugs were applied as indicated in the *Results*. For studies measuring electrically-stimulated [<sup>3</sup>H]DA overflow, slices were field-stimulated for 60 sec (1 Hz, 2 msec delay, 2 msec duration; 0.25-0.30 V per chamber), which was repeated twice during the experiment, 60 min apart. After all samples were collected, individual slices were solubilized in TS-1 (Research Products International; Mount Prospect, IL) for 60 min at 22-25°C to determine the amount of tritium in each slice at the conclusion of the experiment. The amount of radioactivity in all samples was determined by liquid scintillation counting.

**[<sup>3</sup>H]DA uptake into YFP-HA-hDAT-PAE cells.** Specific [<sup>3</sup>H]DA uptake into PAE cells was measured as described (Sorkina et al., 2006). Briefly, cells were incubated with drug in Krebs'-Ringer HEPES buffer (in mM: 120 NaCl, 4.7 KCl, 2.2 CaCl<sub>2</sub>, 1.2 MgSO<sub>4</sub>, 10 glucose, 10 HEPES; pH 7.4) containing ascorbic acid (10 µM), catechol (10 µM) and pargyline (10 µM) for

MOL #56978

30 min at 37°C. Uptake was initiated by the addition of [<sup>3</sup>H]DA (50 nM) for 10 min at 22-25°C. Non-specific [<sup>3</sup>H]DA uptake was determined in the presence of cocaine (1 mM). Cells were washed with Krebs'-Ringer HEPES buffer and solubilized in 0.5 ml 5% trichloroacetic acid for 60 min at 22-25°C. Radioactivity was determined by scintillation counting. Cells from sister wells were solubilized in Triton X-100/glycerol/HEPES lysis buffer for determining protein content by the BCA method.

**Antibody feeding endocytosis assay.** This assay was carried out according to published methods (Sorkina et al., 2006). Briefly, cells, grown on glass coverslips, were pre-incubated with HA11 antibody (1:1000 in binding medium) for 60 min at 22-25°C in the presence of 5% CO<sub>2</sub>, washed and incubated with drug for 30 min at 37°C. Cells were then washed, fixed with fresh 4% paraformaldehyde for 15 min at 22-25°C and stained with the secondary anti-mouse antibody conjugated with Cy5 (1:50 in CMF-PBS + 0.5% BSA) for 60 min at 22-25°C to occupy surface HA11 (i.e. surface hDAT). After washing, cells were permeablized for 5 min with CMF-PBS + 0.5% BSA containing 0.1% saponin before incubating with the same secondary antibody conjugated with Cy3 (1:500 in CMF-PBS + 0.5% BSA containing 0.1% saponin) to label internalized HA11 (i.e. intracellular hDAT). Coverslips were then mounted and analyzed by fluorescence microscopy imaging as previously described (Sorkina et al., 2006).

**Data analyses.** Data are presented as mean values ± SEM (n = number of experiments). All data were analyzed using Prism 5 for Mac OS X (GraphPad; San Diego, CA, USA). For all tests, the threshold for statistical significance was set at the level of  $p < 0.05$ . Concentrations producing half-maximal inhibition (IC<sub>50</sub> values) were determined by variable slope non-linear regression for concentration-response data and by one-site non-linear regression for [<sup>3</sup>H]WIN35,428 binding data. Maximal uptake velocity (V<sub>max</sub>) and substrate affinity (K<sub>m</sub>) were estimated from

MOL #56978

[<sup>3</sup>H]DA/DA uptake kinetic experiments using non-linear regression analyses. Statistical differences between two means were determined by *t*-tests or by one-way or two-way analysis of variance (ANOVA) for differences between more than two means. Paired *t*-tests and repeated measures ANOVAs were used when applicable. When significant effects were observed, one-way and two-way ANOVAs were followed by Bonferroni's multiple-comparisons post-test. Densitometric analyses of immunoblots were performed using NIH Image J (NIH; <http://rsb.info.nih.gov/ij/>). Analyses of biotinylated DATs were carried out as previously described (Hoover et al., 2007). Fractional release of [<sup>3</sup>H]DA was calculated as previously described (Dwoskin and Zahniser, 1986). Peak overflow events following the two periods of stimulation (S1 and S2) were used for calculating the S2/S1 ratios from fractional release experiments. Area under the curve was calculated for fractional release experiments by separately summing events exceeding baseline during the 35 min following S1 (i.e. release above baseline from 20-55 min) and those events exceeding baseline during the 50 min following the initiation of drug superfusion (i.e. release above baseline from 60-110 min).

MOL #56978

## RESULTS

**Cdk5 inhibitors reduce DAT activity in rat dSTR synaptosomes.** We first investigated the time- and concentration-dependent effects of the commonly used Cdk5 inhibitor roscovitine (Meijer et al., 1997) on specific [ $^3$ H]DA uptake into rat dSTR synaptosomes. Roscovitine reduced the specific uptake of [ $^3$ H]DA as early as 5 min (Fig. 1A; 32% decrease). The effect was maximal by 30 min (54% decrease) and persisted through 60 min (Fig. 1A). Two-way ANOVA revealed a significant main effect for treatment ( $F_{1,20} = 210.30$ ,  $p < 0.0001$ ) but not time ( $F_{4,20} = 1.61$ ,  $p < 0.2099$ ). A 30-min incubation time (with no wash out, except where noted) was used for subsequent studies. Roscovitine-mediated decreases in specific [ $^3$ H]DA uptake also occurred in a concentration-dependent manner (Fig. 1B;  $IC_{50} = 31 \mu M$ ). In an additional set of experiments, roscovitine was washed out by twice centrifuging and resuspending the synaptosomes in fresh assay buffer following a 30-min pre-incubation with roscovitine (30  $\mu M$ ). Following drug wash out, specific [ $^3$ H]DA uptake was no longer reduced in these synaptosomes (expressed as % of vehicle-treated control: vehicle,  $100.0 \pm 4.4$ ; roscovitine,  $117.3 \pm 15.5$ ; unpaired  $t$ -test;  $t_{(9)} = 0.65$ ,  $p < 0.5281$ ). Incubation with olomoucine, a less selective yet commonly used Cdk5 inhibitor (Meijer et al., 1997), was equally potent and more efficacious at reducing specific [ $^3$ H]DA uptake (Fig. 1C;  $IC_{50} = 37 \mu M$ ), relative to roscovitine (Fig. 1B). Interestingly, *iso*-olomoucine, a congener of olomoucine that lacks inhibitory activity at Cdk5 ( $IC_{50} > 1 \text{ mM}$ ) (Vesely et al., 1994), decreased specific [ $^3$ H]DA uptake to the same extent and with a similar apparent potency as observed with olomoucine (Fig. 1C). GW8510, a structurally dissimilar inhibitor compared to roscovitine or olomoucine that displays selectivity towards Cdk5 in neuronal tissues (Johnson et al., 2005), also reduced specific [ $^3$ H]DA uptake in a concentration-dependent manner (Fig. 1D). Comparatively, the uptake reducing ability of GW8510 was greater in effect (88% inhibition at

MOL #56978

100  $\mu\text{M}$ ) and more potent ( $\text{IC}_{50} = 7 \mu\text{M}$ ) than the other Cdk5 inhibitors. Specific [ $^3\text{H}$ ]DA uptake was unaffected in samples treated with vehicle (0.1% DMSO or 0.2% DMSO, used only in studies with 100  $\mu\text{M}$  of inhibitor), relative to untreated control samples (data not shown).

We next wanted to test the specificity of the effect of roscovitine on reduced DAT activity. To exclude an effect on generalized membrane-bound transport processes by roscovitine, we incubated dSTR synaptosomes with roscovitine (30  $\mu\text{M}$ ) for 30 min prior to the addition of tritium-labeled amino acids. Roscovitine did not affect the specific uptake of either [ $^3\text{H}$ ]alanine or [ $^3\text{H}$ ]leucine (data not shown). Since roscovitine has been shown to inhibit purified MAPK isoforms with an  $\text{IC}_{50} = 14\text{--}34 \mu\text{M}$  (Meijer et al., 1997) and inhibition of MAPK, which is constitutively active in dSTR synaptosomes, reduces specific [ $^3\text{H}$ ]DA uptake into striatal synaptosomes (Moron et al., 2003), we also measured the levels of phospho-MAPK to determine if similar treatment with roscovitine had any effect on its activation. However, roscovitine did not affect the ratio of phospho-MAPK:total MAPK (data not shown).

We next measured the ability of roscovitine, olomoucine, *iso*-olomoucine and GW8510 to competitively displace binding of the cocaine analog [ $^3\text{H}$ ]WIN35,428 to DATs in rat dSTR membranes. While the DAT inhibitor benztropine almost completely displaced [ $^3\text{H}$ ]WIN35,428 binding (Fig. 2A), increasing concentrations of DMSO (0.00002–0.2%; data not shown) or roscovitine (Fig. 2A) did not decrease [ $^3\text{H}$ ]WIN35,428 binding. In contrast, olomoucine (predicted  $\text{IC}_{50} > 300 \mu\text{M}$ ) and GW8510 (predicted  $\text{IC}_{50} > 100 \mu\text{M}$ ) partially displaced [ $^3\text{H}$ ]WIN35,428 binding (Fig. 2A). *Iso*-olomoucine, the inactive congener of olomoucine, also partially displaced [ $^3\text{H}$ ]WIN35,428 binding and with a slightly higher predicted apparent affinity (predicted  $\text{IC}_{50} > 60 \mu\text{M}$ ) than that observed for olomoucine (Fig. 2A). To exclude a direct interaction of roscovitine with the DAT substrate binding site(s), we also evaluated the effect of

MOL #56978

concomitant exposure to roscovitine (30  $\mu$ M) on displacement of [ $^3$ H]WIN35,428 binding by the DAT substrate AMPH (Fig. 2B). Although AMPH competitively displaced [ $^3$ H]WIN35,428 binding to DATs in dSTR membranes concomitantly exposed to vehicle (0.1% DMSO), roscovitine did not alter this response (AMPH  $IC_{50}$  in the presence of: vehicle, 6  $\mu$ M; roscovitine, 4  $\mu$ M; paired  $t$ -test;  $t_{(11)} = 0.05$ ,  $p < 0.9590$ ). In an effort to circumvent potentially confounding interpretations arising from the putative direct interactions of olomoucine, *iso*-olomoucine and GW8510 with reported DAT binding sites, roscovitine was used exclusively in further studies measuring DAT activity.

### **Cdk5 inhibitors reduce rat dSTR DAT activity via a trafficking-independent mechanism.**

Based on our findings that Cdk5 inhibitors rapidly reduced DAT activity, we investigated whether this was a result of down-regulated cell-surface DAT expression. First, we measured the effect of a 30-min incubation with roscovitine (30  $\mu$ M) on the kinetics of specific [ $^3$ H]DA/DA uptake (Fig. 3A). Roscovitine significantly reduced by 34% (in  $\text{pmol} \cdot \text{min}^{-1} \cdot \text{mg protein}^{-1}$ : vehicle,  $53.8 \pm 7.5$ ; roscovitine,  $35.7 \pm 4.6$ ) the  $V_{\text{max}}$  of specific [ $^3$ H]DA/DA uptake (paired  $t$ -test;  $t_{(2)} = 5.80$ ,  $p < 0.0285$ ). Although pre-incubation with roscovitine caused a 33% increase in  $K_m$  (in nM: control,  $56.2 \pm 4.7$ ; roscovitine,  $83.6 \pm 5.8$ ), this effect was not statistically significant (paired  $t$ -test;  $t_{(2)} = 3.27$ ,  $p < 0.0823$ ). A similar effect on  $V_{\text{max}}$  (34% decrease, paired  $t$ -test;  $t_{(2)} = 6.58$ ,  $p < 0.0223$ ) with a non-significant increase in  $K_m$  (22% increase, paired  $t$ -test;  $t_{(2)} = 3.18$ ,  $p < 0.0862$ ) was also observed following a 15-min incubation with 30  $\mu$ M roscovitine (data not shown). Incubation with vehicle (0.1% DMSO) did not alter the kinetics of specific [ $^3$ H]DA/DA uptake, relative to untreated control samples (data not shown).



MOL #56978

Since decreases in  $V_{\max}$  are suggestive of reduced cell-surface DAT expression, we investigated the effect of roscovitine on cell-surface DAT levels in dSTR synaptosomes by cross-linking surface DATs with sulfo-NHS-biotin. Surprisingly, a 30-min exposure to roscovitine (30  $\mu$ M) failed to alter the level of cell-surface DATs (Fig. 3B; paired  $t$ -test;  $t_{(3)} = 1.09$ ,  $p < 0.3550$ ). Similarly, cell-surface DAT levels in dSTR synaptosomes were unchanged following a 30-min incubation with either 30  $\mu$ M olomoucine or 30  $\mu$ M *iso*-olomoucine (data not shown). Importantly, synaptosomal integrity was maintained throughout the biotinylation procedure as PP2A-A  $\alpha/\beta$ , an intracellular protein, was not detected as being biotinylated under any of the conditions (Fig. 3B). Incubation with vehicle (0.1% DMSO) did not affect the ratio of biotinylated DATs:total DATs, relative to untreated control samples (data not shown).

**Roscovitine does not promote DAT reverse-transport or induce  $\text{Ca}^{2+}$ -dependent [ $^3\text{H}$ ]DA release from rat dSTR slices.** To further explore the effects of Cdk5 inhibitors on DAT activity, we used rat dSTR slices to determine the effect of roscovitine on AMPH-stimulated overflow and non-stimulated outflow of [ $^3\text{H}$ ]DA. After establishing a stable baseline [ $^3\text{H}$ ]DA outflow, slices were stimulated with AMPH (S1; 20  $\mu$ M, 2.5 min) so as to confirm similar magnitudes of [ $^3\text{H}$ ]DA overflow among individual slices (Fig. 4A). Slices were then superfused with vehicle (0.1% DMSO) or 30  $\mu$ M roscovitine (Fig. 4A) for 15 min prior to, but not during, a second stimulation with AMPH (S2; 20  $\mu$ M, 2.5 min). As shown in Fig. 4B, although there was a trend for a concentration-dependent enhancement of AMPH-stimulated [ $^3\text{H}$ ]DA overflow, 30  $\mu$ M roscovitine was the only concentration that produced a significant, ~2-fold elevation in the S2/S1 ratio (one-way ANOVA;  $F_{(3,14)} = 9.71$ ,  $p < 0.0020$ ). The S2/S1 ratio of AMPH-stimulated [ $^3\text{H}$ ]DA overflow (~0.7) was unaffected in slices superfused with vehicle (0.1% DMSO), relative to

MOL #56978

untreated control samples (data not shown). To confirm that the effect of roscovitine was not contingent upon prior exposure to AMPH (20  $\mu$ M) during S1, we also determined the effect of roscovitine in the absence and presence of S1 (Fig. 4C). Fig. 4D shows the summation of fractional [ $^3$ H]DA release (i.e. release over baseline) for these experiments during S1 (left panel) and S2 (right panel). Slices that received the same treatment during the S1 period (20-55 min) did not differ in the magnitude of fractional [ $^3$ H]DA release (Fig. 4D, left panel), but S1 stimulation with AMPH produced a significant increase in [ $^3$ H]DA overflow relative to slices not stimulated with AMPH (one-way ANOVA;  $F_{(3,11)} = 27.06$ ,  $p < 0.0002$ ). Regardless of whether or not slices were stimulated with AMPH at S1, roscovitine superfusion produced a significant increase in the magnitude of S2 AMPH-stimulated [ $^3$ H]DA overflow (Fig. 4D, right panel). Two-way ANOVA revealed significant main effects of drug ( $F_{(1,8)} = 190.4$ ,  $p < 0.0001$ ) and presence or absence of S1 AMPH ( $F_{(1,8)} = 17.36$ ,  $p < 0.0031$ ), as well as an interaction between the two factors ( $F_{(1,8)} = 5.93$ ,  $p < 0.0409$ ).

Since 1) AMPH is a DAT substrate and its ability to promote DAT reverse-transport is sensitive to DAT inhibitors (Sulzer et al., 1995; Kahlig et al., 2005) and 2) roscovitine reduces DAT activity, we hypothesized that concomitant exposure of slices to AMPH (20  $\mu$ M) and roscovitine (30  $\mu$ M) would attenuate AMPH-stimulated [ $^3$ H]DA overflow. As a positive control, we used the DAT inhibitor nomifensine (10  $\mu$ M). Following the first stimulation with AMPH (S1) and 15 min prior to the time of a second stimulation with AMPH (S2; if included), we began superfusion with vehicle or drug (nomifensine or roscovitine) and continued these treatments 15 min beyond S2 (i.e. 30 min total vehicle/drug superfusion). Prior to superfusion with nomifensine, slices showed similar levels of [ $^3$ H]DA overflow following 20  $\mu$ M AMPH-induced S1 (Figs. 5A and 5B; unpaired  $t$ -test;  $t_{(4)} = 0.32$ ,  $p < 0.7683$ ). AMPH-stimulated [ $^3$ H]DA

MOL #56978

overflow was abolished when nomifensine was present during S2 as there was no difference between slices superfused with nomifensine in the absence or presence of S2 (Figs. 5A and 5B; unpaired  $t$ -test;  $t_{(4)} = 1.11$ ,  $p < 0.3295$ ). Surprisingly, however, similar exposure to roscovitine markedly elevated AMPH-stimulated [ $^3\text{H}$ ]DA overflow, relative to slices superfused with vehicle (Fig. 5C). As noted for Figs. 4C and 4D, [ $^3\text{H}$ ]DA overflow was similar among slices receiving the same treatment during the S1 period but different between slices superfused in the absence vs. presence of AMPH (Fig. 5D, left panel; one-way ANOVA;  $F_{(3,11)} = 10.75$ ,  $p < 0.0035$ ). Similar to the 15 min superfusion with roscovitine reported in Fig. 4D, 30 min superfusion with roscovitine produced a significant increase in the magnitude of S2 AMPH-stimulated [ $^3\text{H}$ ]DA overflow (Fig. 5D, right panel), regardless of whether or not slices were stimulated with AMPH at S1. Two-way ANOVA revealed a significant main effect of drug ( $F_{(1,8)} = 80.38$ ,  $p < 0.0001$ ) but not the presence or absence of S1 AMPH ( $F_{(1,8)} = 3.17$ ,  $p < 0.1131$ ), with no interaction between the two factors ( $F_{(1,8)} = 0.48$ ,  $p < 0.5222$ ).

Interestingly, we consistently observed small increases in [ $^3\text{H}$ ]DA overflow as soon as we began to superfuse the dSTR slices with roscovitine (prior to S2; Figs. 4A, 4C and 5C). This observation, taken together with our observation that roscovitine potentiated AMPH-stimulated [ $^3\text{H}$ ]DA overflow (Figs. 4, 5C and 5D), prompted us to next explore the effect of roscovitine, by itself, on [ $^3\text{H}$ ]DA outflow. As observed earlier, similar degrees of AMPH-induced [ $^3\text{H}$ ]DA overflow were observed following S1 (Figs. 6A and 6B; one-way ANOVA;  $F_{(2,11)} = 0.71$ ,  $p < 0.5150$ ). When applied alone, roscovitine (30  $\mu\text{M}$ ) caused a rapid and robust increase in [ $^3\text{H}$ ]DA overflow, which reversed upon cessation of drug superfusion (Figs. 6A and 6B). Next, we wanted to confirm that roscovitine does not promote DAT reverse-transport in dSTR slices. Thus, we measured the effect of concomitant superfusion with nomifensine on roscovitine-

MOL #56978

stimulated [ $^3\text{H}$ ]DA overflow. While nomifensine prevented AMPH-induced reverse-transport of DAT (Fig. 5A), roscovitine-induced [ $^3\text{H}$ ]DA overflow was potentiated by concomitant exposure to nomifensine (Figs. 6A and 6B; one-way ANOVA;  $F_{(2,11)} = 25.77$ ,  $p < 0.0002$ ).

Since roscovitine has been reported to directly enhance activity-dependent neurotransmitter release mediated by P/Q-type calcium channels (Yan et al., 2002), we next determined the calcium-dependency of roscovitine-stimulated [ $^3\text{H}$ ]DA overflow. However, roscovitine-mediated [ $^3\text{H}$ ]DA overflow was still robust when slices were perfused with  $\text{Ca}^{2+}$ -free Krebs' buffer containing EDTA (4  $\mu\text{M}$ ) and EGTA (4  $\mu\text{M}$ ), relative to slices perfused with regular Krebs' buffer containing  $\text{Ca}^{2+}$  (Figs. 6C and 6D). Two-way ANOVA revealed a significant main effect of drug ( $F_{(1,8)} = 176.60$ ,  $p < 0.0001$ ) but not buffer ( $F_{(1,8)} = 2.52$ ,  $p < 0.1511$ ), with no interaction between the two factors ( $F_{(1,8)} = 2.90$ ,  $p < 0.1272$ ). Importantly, similar magnitudes of [ $^3\text{H}$ ]DA overflow were observed following S1 with AMPH, regardless of which buffer was used (one-way ANOVA;  $F_{(3,11)} = 2.54$ ,  $p < 0.1297$ ). In addition, in separate experiments the magnitude of roscovitine-stimulated [ $^3\text{H}$ ]DA overflow was unchanged by electrical stimulation (data not shown).

**Roscovitine reduces hDAT activity in PAE cells via a trafficking-independent mechanism that is likely not mediated by inhibition of Cdk5.** We next used PAE cells stably expressing YFP-HA-hDAT to confirm our finding that roscovitine reduces DAT activity via a trafficking-independent mechanism. To accomplish this, we measured the effect of roscovitine on specific [ $^3\text{H}$ ]DA uptake and on cell-surface hDAT levels, as monitored by endocytosis assays for DAT trafficking (Sorkina et al., 2006). Similar to our observations in dSTR synaptosomes, vehicle (0.1% DMSO) did not affect either specific [ $^3\text{H}$ ]DA uptake or cell-surface hDAT levels in PAE

MOL #56978

cells (data not shown). Following a 30-min incubation of cells with roscovitine (30  $\mu$ M), specific [ $^3$ H]DA uptake was significantly reduced by 35% (Fig. 7A; repeated measures one-way ANOVA;  $F_{(2,8)} = 22.85$ ,  $p < 0.0065$ ). As a positive control, we also exposed PAE cells to the phorbol ester PMA (1  $\mu$ M), which we have previously shown to down-regulate PAE hDAT activity (Sorkina et al., 2005). Following a 30-min PMA incubation, specific [ $^3$ H]DA uptake was significantly reduced by 49% (Fig. 7A).

To test whether roscovitine-induced reduction of specific [ $^3$ H]DA uptake was due to accelerated endocytosis of DATs, the HA11 endocytosis assay was performed in YFP-HA-hDAT-PAE cells as described by Sorkina and colleagues (2006). In these experiments, endosomes containing internalized HA11:YFP-HA-hDAT complexes were identified by Cy3 fluorescence that co-localizes with YFP fluorescence, but that does not co-localize with Cy5 fluorescence (the latter corresponds to YFP-HA-hDAT at the plasma membrane). As seen in Fig. 7B, PMA treatment resulted in the appearance of a large number of endosomes containing endocytosed YFP-HA-hDAT. In contrast to PMA, a 30-min incubation with roscovitine (30  $\mu$ M) did not alter the distribution of Cy5, Cy3 or YFP fluorescence, relative to vehicle-treated cells (Fig. 7B), again suggesting that roscovitine does not accelerate hDAT endocytosis or down-regulate cell-surface hDAT expression.

To determine if roscovitine-induced decreases in hDAT activity were, in fact, Cdk5-mediated, we transfected YFP-HA-hDAT expressing PAE cells with siRNA targeted against Cdk5. Seventy-two hours post-transfection with 25 nM, 50 nM or 100 nM Cdk5-siRNA, Cdk5 protein levels were significantly reduced by 83%, 86% and 79%, respectively (Fig. 8A; one-way ANOVA;  $F_{(3,15)} = 10.15$ ,  $p < 0.0013$ ), relative to cells transfected with NT-siRNA. We next determined whether similar Cdk5-siRNA transfections diminished the effect of roscovitine (30

MOL #56978

$\mu\text{M}$ ) on specific [ $^3\text{H}$ ]DA uptake into hDAT-PAE cells (Fig. 8B). Repeated measures two-way ANOVA revealed a significant main effect of drug treatment ( $F_{(1,8)} = 54.43$ ,  $p < 0.0001$ ) but not siRNA treatment ( $F_{(3,8)} = 0.32$ ,  $p < 0.8135$ ), with no interaction between the two factors ( $F_{(3,8)} = 0.86$ ,  $p < 0.4983$ ). Consistent with our earlier finding (Fig. 7A), a 30-min incubation with roscovitine (30  $\mu\text{M}$ ) significantly decreased specific [ $^3\text{H}$ ]DA uptake by 48% in cells transfected with NT-siRNA (Fig. 8B). Roscovitine significantly decreased specific [ $^3\text{H}$ ]DA uptake by 49% and 61% in cells transfected with 50 nM and 100 nM Cdk5-siRNA, respectively, but not with 25 nM Cdk5-siRNA, which reduced [ $^3\text{H}$ ]DA uptake by 32%. Although Cdk5-siRNA did not affect the [ $^3\text{H}$ ]DA uptake response (Fig. 8B), we note that enhanced variability was seen in vehicle-treated cells transfected with Cdk5-siRNA (Fig. 8B). NT-siRNA did not affect the level of Cdk5 protein or specific [ $^3\text{H}$ ]DA uptake, relative to non-transfected cells (data not shown).

MOL #56978

## DISCUSSION

Several protein kinases and their inhibitors rapidly regulate DAT trafficking and/or activity. Cdk5 is found in nigrostriatal DA neurons (Smith et al., 2003; Chergui et al., 2004), but whether or not it regulates brain DATs had not previously been reported. Here, we show for the first time that: 1) Cdk5 inhibitors reduce DAT activity via a mechanism that is independent of DAT trafficking and reverse-transport; 2) the Cdk5 inhibitor roscovitine induces spontaneous [<sup>3</sup>H]DA release from dSTR slices; but 3) the ability of roscovitine to reduce DAT activity is, most likely, independent of Cdk5 inhibition. Therefore, when using such inhibitors, mechanistic conclusions must be drawn with caution. Nevertheless, our findings further support the idea that Cdk5 inhibitors can affect the disposition of DA at the level of striatal DA nerve terminals.

Roscovitine and olomoucine, two commonly used Cdk5 inhibitors, decrease purified Cdk5 activity with IC<sub>50</sub> values of 0.16 μM and 3 μM, respectively (Meijer et al., 1997) whereas the structurally dissimilar inhibitor GW8510 reduces neuronal apoptosis with a predicted IC<sub>50</sub> < 1 μM (Johnson et al., 2005). Here, roscovitine, olomoucine and GW8510 all reduced specific [<sup>3</sup>H]DA uptake into dSTR synaptosomes in a rapid, concentration-dependent manner, but with somewhat lower potencies than reported for Cdk5 inhibition (IC<sub>50</sub> values in μM: 31, 37 and 7, respectively). With the exception of roscovitine, the ability of Cdk5 inhibitors to reduce specific [<sup>3</sup>H]DA uptake was potentially confounded by our finding that concentrations of these inhibitors that reduced [<sup>3</sup>H]DA uptake also competed with the cocaine analog [<sup>3</sup>H]WIN35,428 for binding to DATs, suggesting a direct interaction. Also, *iso*-olomoucine, IC<sub>50</sub> > 1 mM for inhibiting Cdk5 activity (Vesely et al., 1994), reduced specific [<sup>3</sup>H]DA uptake with a similar apparent potency as olomoucine and displaced [<sup>3</sup>H]WIN35,428 binding to DATs. Thus, this limited the utility of the inactive congener of olomoucine for determining the Cdk5 selectivity of olomoucine. In any

MOL #56978

case, a direct interaction with DAT cocaine binding sites by olomoucine, *iso*-olomoucine and GW8510 likely contributes to their ability to reduce DAT activity, irrespective of any inhibition of Cdk5. On the other hand, this was not the case for roscovitine, which failed to reduce [<sup>3</sup>H]WIN35,428 binding or affect AMPH displacement of [<sup>3</sup>H]WIN35,428 binding. Although roscovitine does not interact with the DAT cocaine or substrate binding sites, roscovitine may regulate DAT activity through an allosteric binding site, as reduced [<sup>3</sup>H]DA uptake was no longer observed following roscovitine wash out.

The roscovitine-mediated reduction of DAT activity seen following a 15- or 30-min pre-incubation was explained by a significant decrease in the  $V_{\max}$  of specific DAT-mediated uptake into dSTR synaptosomes. One prominent mechanism of rapid DAT regulation, which is consistent with a reduction in  $V_{\max}$ , is altered DAT trafficking to and from the plasma membrane (Zahniser and Sorkin, 2009). Thus, we were surprised that neither roscovitine nor olomoucine altered cell-surface DAT levels, as measured by either biotinylation assays in dSTR synaptosomes or single-cell endocytosis assays in YFP-HA-hDAT-PAE cells. Based on these findings, it seems likely that roscovitine alters the intrinsic transport properties of DATs.

Our results using dSTR slices showed that 30  $\mu$ M roscovitine alone produced a robust, reversible [<sup>3</sup>H]DA overflow, which was not inhibited by the DAT inhibitor nomifensine, but rather was additive with nomifensine. These data indicate that the ability of roscovitine to stimulate [<sup>3</sup>H]DA overflow from dSTR slices is independent of DAT reverse-transport. Further, concomitant superfusion with roscovitine and AMPH potentiated AMPH-stimulated [<sup>3</sup>H]DA overflow (S2) in dSTR slices independent of whether or not slices were previously superfused with AMPH at S1. These observations, thus, revealed additional differences between nomifensine and roscovitine because, unlike nomifensine, roscovitine did not block AMPH-



MOL #56978

stimulated [ $^3\text{H}$ ]DA overflow. In light of our findings with [ $^3\text{H}$ ]DA uptake into dSTR synaptosomes, the most parsimonious explanation for our observations is that in the presence of roscovitine a significant proportion of dSTR DAT molecules continue to function normally, transporting AMPH and DA. Indeed, specific [ $^3\text{H}$ ]DA uptake was only reduced by ~55% with the highest concentration of roscovitine tested (100  $\mu\text{M}$ ). Based on potency, relatively high concentrations of roscovitine ( $\text{IC}_{50} = 31 \mu\text{M}$ ) would be expected to be less effective at reducing DAT activity, as compared with the prototypical DAT inhibitors, cocaine ( $\text{IC}_{50} = 310 \text{ nM}$ ) or nomifensine ( $\text{IC}_{50} = 48 \text{ nM}$ ) (Hyttel, 1982).

Roscovitine has been reported to directly activate P/Q-type  $\text{Ca}^{2+}$  channels (Yan et al., 2002) and to potentiate electrically-stimulated release of DA from striatal slices (Chergui et al., 2004). Interestingly, the roscovitine-stimulated [ $^3\text{H}$ ]DA overflow we observed in dSTR slices persisted when slices were perfused with  $\text{Ca}^{2+}$ -free buffer and was not altered by electrical stimulation, suggesting that in our assays roscovitine did not affect activity-dependent [ $^3\text{H}$ ]DA release. The reason for these differences may be the result of different experimental methodologies/conditions between our study and those of the two aforementioned studies. Importantly, like cocaine, roscovitine appeared to prolong DA clearance in the study by Chergui and colleagues (2004). Although, the effects of Cdk5 inhibitors on DAT activity appear to be independent of DAT reverse-transport, intracellular sodium is required for AMPH-induced efflux of DA via DAT (Kahlig et al., 2005). To the best of our knowledge, with the exception of P/Q-type calcium channel-roscovitine interaction (Yan et al., 2002), the effects of Cdk5 inhibitors on membrane voltage and/or ionic carriers such as the Na,K-ATPase have not been studied. If such effects do exist, these would potentially impact DAT activity (Sonders et al., 1997). Taken together, our findings are consistent with roscovitine elevating spontaneous,  $\text{Ca}^{2+}$ -independent release of

MOL #56978

[<sup>3</sup>H]DA, an effect that is exacerbated by the ability of roscovitine to prevent the re-accumulation of recently released [<sup>3</sup>H]DA by reducing DAT activity.

Inhibition of MAPK reduces specific [<sup>3</sup>H]DA uptake into striatal synaptosomes by down-regulating cell-surface DAT levels (Moron et al., 2003). Although roscovitine can potentially inhibit MAPK isoforms (Meijer et al., 1997), roscovitine did not alter phospho-MAPK levels or cell-surface DAT levels. These findings suggest that the effects of roscovitine on DAT activity are mediated by a MAPK-independent mechanism. Similar to MAPK, inhibition of insulin signaling down-regulates DAT activity by reducing the number of functional cell-surface DATs (Carvelli et al., 2002; Garcia et al., 2005). Although roscovitine reduces the activity of purified insulin-receptor tyrosine kinase with an IC<sub>50</sub> = 70 μM (Meijer et al., 1997), the roscovitine effect on [<sup>3</sup>H]DA uptake was more potent and occurred via a trafficking-independent mechanism. Thus, it is unlikely that the effect of roscovitine is mediated through inhibition of insulin receptors.

Recently, Cdk5 has been shown to increase phosphorylation of the recombinantly-expressed DAT N-terminal tail (Gorentla et al., 2009). To determine if the pharmacological actions of roscovitine on DAT activity we observed were Cdk5-mediated, we transfected YFP-HA-hDAT-PAE cells with Cdk5-siRNA. Although up to 86% knock-down of Cdk5 protein levels was achieved, transfection with Cdk5-siRNA did not alter specific [<sup>3</sup>H]DA uptake into PAE cells. Furthermore, a 32-61% roscovitine-induced reduction in specific [<sup>3</sup>H]DA uptake, similar to that in control cells, was still observed in Cdk5-siRNA-transfected cells. Although there was increased variability of specific [<sup>3</sup>H]DA uptake into vehicle-treated cells transfected with Cdk5-siRNA, Cdk5-siRNA did not affect [<sup>3</sup>H]DA uptake *per se*. These findings suggest that it is unlikely that the ability of roscovitine to reduce hDAT activity is mediated by inhibition of Cdk5

MOL #56978

and further suggest that roscovitine inhibits DAT activity through an alternative mechanism (e.g. an allosteric binding site). Nonetheless, the possibility remains that compensatory changes may take place in the seventy-two hours between transfection and experimentation, which may mask effects due to loss of Cdk5.

Our study demonstrates that Cdk5 inhibitors, and in particular roscovitine, reduce DAT activity via a mechanism(s) that is independent of DAT trafficking and reverse-transport. These effects, most likely, occur in a Cdk5-independent manner and may involve changes in the intrinsic transport properties of DATs through direct and/or indirect interaction(s). Thus, the molecular mechanism(s) by which these Cdk5 inhibitors impact DA neurotransmission must be interpreted with caution. Potentially, Cdk5-deficient would be a useful model for exploring the question of Cdk5 involvement further, but these mice die shortly after birth and display neurodevelopmental abnormalities (Dhavan and Tsai, 2001). In any case, the use of p35-deficient mice, which lack this neuronal activator of Cdk5, and genetic models with modified Cdk5 activity within select neuronal populations will continue to be instrumental for uncovering the role of Cdk5 in DA-related disease states (Benavides et al., 2007).

MOL #56978

## ACKNOWLEDGEMENTS

We would like to thank Mr. Gaynor Larson (*University of Colorado Denver*) for expert technical assistance, Ms. Tatiana Sorkina (*University of Colorado Denver*) for providing YFP-HA-hDAT expressing PAE cells and helpful discussions and Dr. Richard M. Allen (*University of Colorado Denver*) for helpful discussions regarding statistical analyses.

MOL #56978

## REFERENCES

- Benavides DR, Quinn JJ, Zhong P, Hawasli AH, Dileone RJ, Kansy JW, Olausson P, Yan Z, Taylor JR and Bibb JA (2007) Cdk5 Modulates Cocaine Reward, Motivation, and Striatal Neuron Excitability. *J Neurosci* **27**:12967-12976.
- Bibb JA, Chen J, Taylor JR, Svenningsson P, Nishi A, Snyder GL, Yan Z, Sagawa ZK, Ouimet CC, Nairn AC, Nestler EJ and Greengard P (2001) Effects of chronic exposure to cocaine are regulated by the neuronal protein Cdk5. *Nature* **410**:376-380.
- Bibb JA, Snyder GL, Nishi A, Yan Z, Meijer L, Fienberg AA, Tsai LH, Kwon YT, Girault JA, Czernik AJ, Huganir RL, Hemmings HC, Jr., Nairn AC and Greengard P (1999) Phosphorylation of DARPP-32 by Cdk5 modulates dopamine signalling in neurons. *Nature* **402**:669-671.
- Blakely RD and Bauman AL (2000) Biogenic amine transporters: regulation in flux. *Curr Opin Neurobiol* **10**:328-336.
- Bradford MM (1976) A rapid and sensitive method for the quantitation of microgram quantities of protein utilizing the principle of protein-dye binding. *Anal Biochem* **72**:248-254.
- Carvelli L, Moron JA, Kahlig KM, Ferrer JV, Sen N, Lechleiter JD, Leeb-Lundberg LM, Merrill G, Lafer EM, Ballou LM, Shippenberg TS, Javitch JA, Lin RZ and Galli A (2002) PI 3-kinase regulation of dopamine uptake. *J Neurochem* **81**:859-869.
- Chen R, Furman CA, Zhang M, Kim MN, Gereau RWt, Leitges M and Gnegy ME (2009) Protein kinase C $\beta$  is a critical regulator of dopamine transporter trafficking and regulates the behavioral response to amphetamine in mice. *J Pharmacol Exp Ther* **328**:912-920.

MOL #56978

- Chen R, Tilley MR, Wei H, Zhou F, Zhou FM, Ching S, Quan N, Stephens RL, Hill ER, Nottoli T, Han DD and Gu HH (2006) Abolished cocaine reward in mice with a cocaine-insensitive dopamine transporter. *Proc Natl Acad Sci U S A* **103**:9333-9338.
- Chergui K, Svenningsson P and Greengard P (2004) Cyclin-dependent kinase 5 regulates dopaminergic and glutamatergic transmission in the striatum. *Proc Natl Acad Sci U S A* **101**:2191-2196.
- Coffey LL and Reith ME (1994) [3H]WIN 35,428 binding to the dopamine uptake carrier. I. Effect of tonicity and buffer composition. *J Neurosci Methods* **51**:23-30.
- Daniels GM and Amara SG (1999) Regulated trafficking of the human dopamine transporter. Clathrin-mediated internalization and lysosomal degradation in response to phorbol esters. *J Biol Chem* **274**:35794-35801.
- Dhavan R and Tsai LH (2001) A decade of CDK5. *Nat Rev Mol Cell Biol* **2**:749-759.
- Dwoskin LP and Zahniser NR (1986) Robust modulation of [3H]dopamine release from rat striatal slices by D-2 dopamine receptors. *J Pharmacol Exp Ther* **239**:442-453.
- Fog JU, Khoshbouei H, Holy M, Owens WA, Vaegter CB, Sen N, Nikandrova Y, Bowton E, McMahon DG, Colbran RJ, Daws LC, Sitte HH, Javitch JA, Galli A and Gether U (2006) Calmodulin kinase II interacts with the dopamine transporter C terminus to regulate amphetamine-induced reverse transport. *Neuron* **51**:417-429.
- Foster JD, Cervinski MA, Gorentla BK and Vaughan RA (2006) Regulation of the dopamine transporter by phosphorylation. *Handb Exp Pharmacol*:197-214.
- Garcia BG, Wei Y, Moron JA, Lin RZ, Javitch JA and Galli A (2005) Akt is essential for insulin modulation of amphetamine-induced human dopamine transporter cell-surface redistribution. *Mol Pharmacol* **68**:102-109.

MOL #56978

- Giros B, Jaber M, Jones SR, Wightman RM and Caron MG (1996) Hyperlocomotion and indifference to cocaine and amphetamine in mice lacking the dopamine transporter. *Nature* **379**:606-612.
- Gorentla BK, Moritz AE, Foster JD and Vaughan RA (2009) Proline-directed phosphorylation of the dopamine transporter N-terminal domain. *Biochemistry* **48**:1067-1076.
- Hoover BR, Everett CV, Sorkin A and Zahniser NR (2007) Rapid regulation of dopamine transporters by tyrosine kinases in rat neuronal preparations. *J Neurochem* **101**:1258-1271.
- Hyttel J (1982) Citalopram--pharmacological profile of a specific serotonin uptake inhibitor with antidepressant activity. *Prog Neuropsychopharmacol Biol Psychiatry* **6**:277-295.
- Johnson K, Liu L, Majdzadeh N, Chavez C, Chin PC, Morrison B, Wang L, Park J, Chugh P, Chen HM and D'Mello SR (2005) Inhibition of neuronal apoptosis by the cyclin-dependent kinase inhibitor GW8510: identification of 3' substituted indolones as a scaffold for the development of neuroprotective drugs. *J Neurochem* **93**:538-548.
- Kahlig KM, Binda F, Khoshbouei H, Blakely RD, McMahon DG, Javitch JA and Galli A (2005) Amphetamine induces dopamine efflux through a dopamine transporter channel. *Proc Natl Acad Sci U S A* **102**:3495-3500.
- Kansy JW, Daubner SC, Nishi A, Sotogaku N, Lloyd MD, Nguyen C, Lu L, Haycock JW, Hope BT, Fitzpatrick PF and Bibb JA (2004) Identification of tyrosine hydroxylase as a physiological substrate for Cdk5. *J Neurochem* **91**:374-384.
- Meijer L, Borgne A, Mulner O, Chong JP, Blow JJ, Inagaki N, Inagaki M, Delcros JG and Moulinoux JP (1997) Biochemical and cellular effects of roscovitine, a potent and selective inhibitor of the cyclin-dependent kinases cdc2, cdk2 and cdk5. *Eur J Biochem* **243**:527-536.

MOL #56978

- Melikian HE and Buckley KM (1999) Membrane trafficking regulates the activity of the human dopamine transporter. *J Neurosci* **19**:7699-7710.
- Moron JA, Zakharova I, Ferrer JV, Merrill GA, Hope B, Lafer EM, Lin ZC, Wang JB, Javitch JA, Galli A and Shippenberg TS (2003) Mitogen-activated protein kinase regulates dopamine transporter surface expression and dopamine transport capacity. *J Neurosci* **23**:8480-8488.
- Moy LY and Tsai LH (2004) Cyclin-dependent kinase 5 phosphorylates serine 31 of tyrosine hydroxylase and regulates its stability. *J Biol Chem* **279**:54487-54493.
- Nirenberg MJ, Vaughan RA, Uhl GR, Kuhar MJ and Pickel VM (1996) The dopamine transporter is localized to dendritic and axonal plasma membranes of nigrostriatal dopaminergic neurons. *J Neurosci* **16**:436-447.
- Pristupa ZB, McConkey F, Liu F, Man HY, Lee FJ, Wang YT and Niznik HB (1998) Protein kinase-mediated bidirectional trafficking and functional regulation of the human dopamine transporter. *Synapse* **30**:79-87.
- Schultz W (2007) Multiple dopamine functions at different time courses. *Annu Rev Neurosci* **30**:259-288.
- Smith PD, Crocker SJ, Jackson-Lewis V, Jordan-Sciutto KL, Hayley S, Mount MP, O'Hare MJ, Callaghan S, Slack RS, Przedborski S, Anisman H and Park DS (2003) Cyclin-dependent kinase 5 is a mediator of dopaminergic neuron loss in a mouse model of Parkinson's disease. *Proc Natl Acad Sci U S A* **100**:13650-13655.
- Sonders MS, Zhu SJ, Zahniser NR, Kavanaugh MP and Amara SG (1997) Multiple ionic conductances of the human dopamine transporter: the actions of dopamine and psychostimulants. *J Neurosci* **17**:960-974.



MOL #56978

- Sorkina T, Hoover BR, Zahniser NR and Sorkin A (2005) Constitutive and protein kinase C-induced internalization of the dopamine transporter is mediated by a clathrin-dependent mechanism. *Traffic* **6**:157-170.
- Sorkina T, Miranda M, Dionne KR, Hoover BR, Zahniser NR and Sorkin A (2006) RNA interference screen reveals an essential role of Ned4-2 in dopamine transporter ubiquitination and endocytosis. *J Neurosci* **26**:8195-8205.
- Sulzer D, Chen TK, Lau YY, Kristensen H, Rayport S and Ewing A (1995) Amphetamine redistributes dopamine from synaptic vesicles to the cytosol and promotes reverse transport. *J Neurosci* **15**:4102-4108.
- Taylor JR, Lynch WJ, Sanchez H, Olausson P, Nestler EJ and Bibb JA (2007) Inhibition of Cdk5 in the nucleus accumbens enhances the locomotor-activating and incentive-motivational effects of cocaine. *Proc Natl Acad Sci U S A* **104**:4147-4152.
- Vesely J, Havlicek L, Strnad M, Blow JJ, Donella-Deana A, Pinna L, Letham DS, Kato J, Detivaud L, Leclerc S and et al. (1994) Inhibition of cyclin-dependent kinases by purine analogues. *Eur J Biochem* **224**:771-786.
- Yan Z, Chi P, Bibb JA, Ryan TA and Greengard P (2002) Roscovitine: a novel regulator of P/Q-type calcium channels and transmitter release in central neurons. *J Physiol* **540**:761-770.
- Zahniser NR and Sorkin A (2009) Trafficking of dopamine transporters in psychostimulant actions. *Seminars Cell Develop Biol* **20**:411-417.
- Zheng M, Leung CL and Liem RK (1998) Region-specific expression of cyclin-dependent kinase 5 (cdk5) and its activators, p35 and p39, in the developing and adult rat central nervous system. *J Neurobiol* **35**:141-159.

MOL #56978

This work was supported by the National Institutes of Health, National Institute on Drug Abuse [Grants F32 DA025397, DA004216, DA015050, DA014204].

Primary Laboratory of Origin: Nancy R. Zahniser

This work was previously presented at the annual meeting of the *Society for Neuroscience*: Price DA, Sorkina T, Sorkin A and Zahniser NR (2008) Rapid regulation of rat brain dopamine transporter by cyclin-dependent kinase 5 inhibitors. *Society for Neuroscience*, 134.19.

Reprint Requests: Dr. David A. Price, University of Colorado Denver, Department of Pharmacology Mail Stop 8303 RC1-North Tower, 12800 E. 19<sup>th</sup> Ave P18-6402K, Aurora, CO 80045

MOL #56978

## FIGURE LEGENDS

**Fig. 1.** Cdk5 inhibitors reduced specific [ $^3$ H]DA uptake into rat dSTR synaptosomes. Synaptosomes were incubated with drug at 37°C, and specific uptake of 0.5 nM [ $^3$ H]DA was measured. A, Effect of incubation with roscovitine (30  $\mu$ M) for increasing periods of time on specific [ $^3$ H]DA uptake. \*\*\* $p$ <0.001 compared to respective vehicle-treated control (two-way ANOVA followed by Bonferroni's multiple-comparisons post-test). B-D, Concentration-response curves of specific [ $^3$ H]DA uptake following a 30-min incubation with roscovitine, olomoucine or *iso*-olomoucine or GW8510. Data represent mean values  $\pm$  SEM for  $n = 3$  independent experiments, each performed in triplicate. Dashed line represents vehicle (0.1% DMSO) control.

**Fig. 2.** Differential effects of Cdk5 inhibitors were observed on steady-state [ $^3$ H]WIN35,428 binding to DATs in rat dSTR membranes. A, The ability of increasing concentrations of roscovitine, olomoucine, *iso*-olomoucine and GW8510 to compete with 4 nM [ $^3$ H]WIN35,428 binding is shown. Non-specific binding is shown in the presence of the DAT inhibitor benztropine (2.4  $\mu$ M). B, Concomitant exposure to roscovitine (30  $\mu$ M) did not alter the ability of AMPH to compete with 4 nM [ $^3$ H]WIN35,428 binding in dSTR membranes. Data represent mean values  $\pm$  SEM for  $n = 3$ -4 independent experiments, each performed in triplicate. Dashed line represents vehicle (0.1% DMSO) control.

**Fig. 3.** Roscovitine reduced the  $V_{\max}$  of specific [ $^3$ H]DA/DA uptake into rat dSTR synaptosomes via a trafficking-independent mechanism. A, Effect of a 30-min incubation of dSTR synaptosomes with roscovitine (30  $\mu$ M) on the kinetics of specific [ $^3$ H]DA/DA uptake. See

MOL #56978

*Results* for  $V_{\max}$  and  $K_m$  values. Data represent mean values  $\pm$  SEM for  $n = 3$  independent experiments, each performed in triplicate. B, Following an identical exposure to roscovitine, cell-surface DAT number was estimated in dSTR synaptosomes by using sulfo-NHS-biotin labeling. Top panel: representative immunoblots of total (T) and biotinylated (B) DAT and PP2A- $\alpha/\beta$ . Bottom panel: bands were quantified by densitometry. Data represent mean  $\pm$  SEM for  $n=4$  independent experiments.

**Fig. 4.** Prior superfusion with roscovitine potentiated AMPH-stimulated [ $^3$ H]DA overflow from rat dSTR slices. Slices were pre-loaded with [ $^3$ H]DA (0.1  $\mu$ M) and spontaneous [ $^3$ H]DA outflow was allowed to stabilize for 75 min at 35°C. Subsequently, [ $^3$ H]DA overflow was stimulated by exposure to AMPH (20  $\mu$ M) for 2.5 min at S1 and S2, as indicated (see *Materials and Methods*). A and C, Inclusion of vehicle (0.1% DMSO) or roscovitine (30  $\mu$ M) is indicated by bars below the  $x$ -axes labeled “Rx”. Data represent mean values  $\pm$  SEM for  $n=3$  independent experiments, each performed in duplicate. A, Time course for the effect of roscovitine added to the superfusion buffer 15 min before S2 on AMPH-stimulated [ $^3$ H]DA overflow. B, Overall results from experiments similar to those in *panel A* showing the effect of a 15-min pre-exposure to increasing concentrations of roscovitine on the S2/S1 ratio (AMPH-stimulated [ $^3$ H]DA overflow following S1 and S2). \*\*\* $p<0.0001$  compared to 0  $\mu$ M roscovitine (0.1% DMSO; one-way ANOVA followed by Bonferroni’s multiple-comparisons post-test). Data represent mean values  $\pm$  SEM for  $n = 3-5$  independent experiments, each performed in duplicate. C, Time course for the effect of 15 min superfusion with roscovitine on S2 AMPH-stimulated [ $^3$ H]DA overflow in the absence or presence of AMPH-stimulation at S1. D, Summation of fractional release of [ $^3$ H]DA from *panel C* during the 35 min following S1 (*left panel*; 20-55 min in *4C*) and again during the

MOL #56978

50 min following the initiation of drug superfusion (*right panel*; 60-110 min in *4C*). Release above baseline occurring from 20-55 min was analyzed by one-way ANOVA and by two-way ANOVA for that occurring from 50-110 min.  $**p<0.01$  and  $***p<0.001$  as shown (Bonferroni's multiple-comparisons post-test).

**Fig. 5.** Concomitant superfusion with the DAT inhibitor nomifensine prevented AMPH-induced [ $^3\text{H}$ ]DA overflow from rat dSTR slices whereas superfusion with roscovitine potentiated it. See *Fig. 4* for experimental details. Vehicle (0.1% DMSO) or drug (10  $\mu\text{M}$  nomifensine or 30  $\mu\text{M}$  roscovitine) were applied for 30 min as shown (bar below *x*-axes labeled "Rx"). Data represent mean values  $\pm$  SEM for  $n = 3$  independent experiments, each performed in duplicate. A, Time course for the effect of nomifensine on AMPH-stimulated [ $^3\text{H}$ ]DA overflow in the absence or presence of S2. B, Summation of fractional release of [ $^3\text{H}$ ]DA from *panel A*, as described in *Fig. 4D*. C, Time course for the effect of roscovitine on S2 AMPH-stimulated [ $^3\text{H}$ ]DA overflow with or without AMPH-stimulation at S1 showed similar results to *Fig. 4C*. D, Summation of fractional release of [ $^3\text{H}$ ]DA from *panel C* was analyzed as described in *Fig. 4D*.  $*p<0.05$ ,  $**p<0.01$  and  $***p<0.001$  as shown (Bonferroni's multiple-comparisons post-test).

**Fig. 6.** Roscovitine-mediated [ $^3\text{H}$ ]DA overflow from rat dSTR slices was independent of DAT reverse-transport, enhanced by nomifensine and  $\text{Ca}^{2+}$ -independent. Slices were prepared as in *Fig. 4*. [ $^3\text{H}$ ]DA overflow was stimulated by exposure to AMPH (20  $\mu\text{M}$ ) for 2.5 min at S1. Vehicle (0.1% DMSO) or drug(s) were applied for 30 min (A) or 15 min (B) as shown (bar below *x*-axes labeled "Rx"). Data represent mean values  $\pm$  SEM for  $n = 3$  independent experiments, each performed in duplicate. A, Time course for the effect of roscovitine and

MOL #56978

nomifensine, alone or together, on [ $^3$ H]DA overflow. B, Summation of fractional release of [ $^3$ H]DA data from *panel A*, as described in *Fig. 4D*.  $**p<0.01$  as shown (one-way ANOVA followed by Bonferroni's multiple-comparisons post-test). C, Time course for the effect of continuous perfusion with Krebs' buffer vs.  $\text{Ca}^{2+}$ -free Krebs' buffer containing EDTA (4  $\mu\text{M}$ ) and EGTA (4  $\mu\text{M}$ ) on roscovitine-induced [ $^3$ H]DA overflow. D, Summation of fractional release of [ $^3$ H]DA data from *panel C* was analyzed as described in *Fig. 4D*.  $***p<0.001$  as shown (Bonferroni's multiple-comparisons post-test).

**Fig. 7.** Roscovitine reduced hDAT activity via a trafficking-independent mechanism in PAE cells stably expressing YFP-HA-hDAT. A, Cells were incubated with roscovitine or PMA for 30 min at 37°C, and hDAT-mediated specific uptake of 50 nM [ $^3$ H]DA (10 min at 22-25°C) was measured. Dashed line represents vehicle (0.1% DMSO) control. Data represent mean values  $\pm$  SEM for  $n = 3$  independent experiments, each performed in triplicate.  $*p<0.05$  and  $**p<0.01$  compared to vehicle (repeated measures one-way ANOVA followed by Bonferroni's multiple comparisons post-test). B, Representative images of YFP-HA-hDAT expressing PAE cells exposed to vehicle, roscovitine or PMA for 30 min at 37°C after pre-binding HA11 for 60 min at 22-25°C. Staining was performed as described (see *Materials and Methods*). Examples in high-magnification insets demonstrate the absence (vehicle and roscovitine) or presence (PMA) of YFP-HA-hDAT containing endosomes (co-localization of YFP and Cy3 fluorescence and the absence of Cy5 fluorescence). Scale bar = 10  $\mu\text{m}$ .

**Fig. 8.** Roscovitine likely reduced [ $^3$ H]DA uptake into YFP-HA-hDAT PAE cells in a Cdk5 independent manner. PAE cells stably expressing YFP-HA-hDAT were transfected with NT-

MOL #56978

siRNA or increasing concentrations of Cdk5-siRNA as described (see *Materials and Methods*). Cells were processed for experiments seventy-two hours post-transfection. A, Effect of increasing concentrations of Cdk5-siRNA on PAE Cdk5 protein levels are shown. Top panel: representative immunoblots of Cdk5 and  $\beta$ -actin. Bottom panel: bands were quantified by densitometry. Data represent mean values  $\pm$  SEM for  $n=3$  independent experiments.  $**p<0.01$  compared to cells transfected with NT-siRNA (one-way ANOVA followed by Bonferroni's multiple-comparisons post-test). B, Specific [ $^3$ H]DA uptake into PAE cells was measured in the absence or presence of roscovitine (30  $\mu$ M) from cells transfected with increasing concentrations of Cdk5-siRNA. Data are presented as a scatter plot with individual symbols representing the average from an independent experiment performed in duplicate. Solid lines represent the mean for the  $n = 3$  independent experiments for each condition. Dashed line represents vehicle (0.1% DMSO) control.  $*p<0.05$  and  $**p<0.01$  compared to respective vehicle control (repeated measures two-way ANOVA followed by Bonferroni's multiple-comparisons post-test).

**Figure 1**

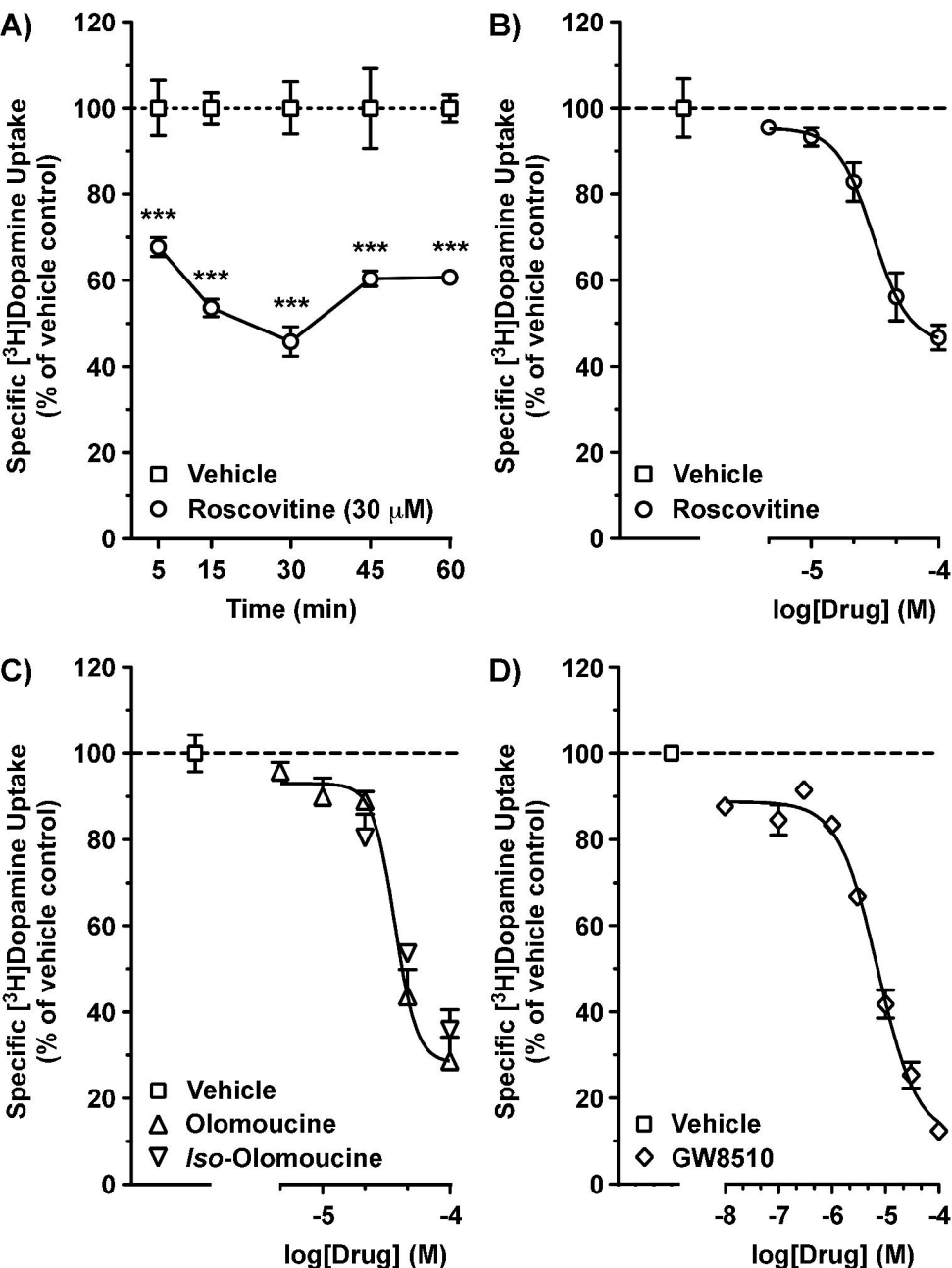




**Figure 2**

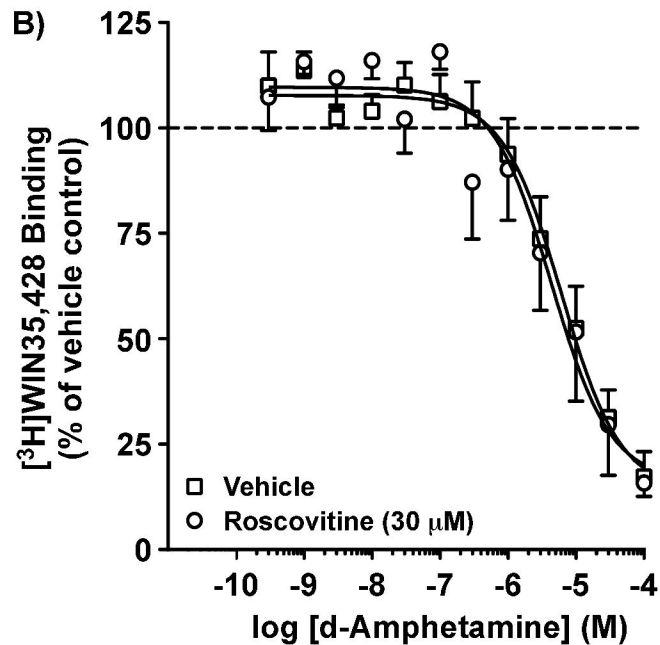
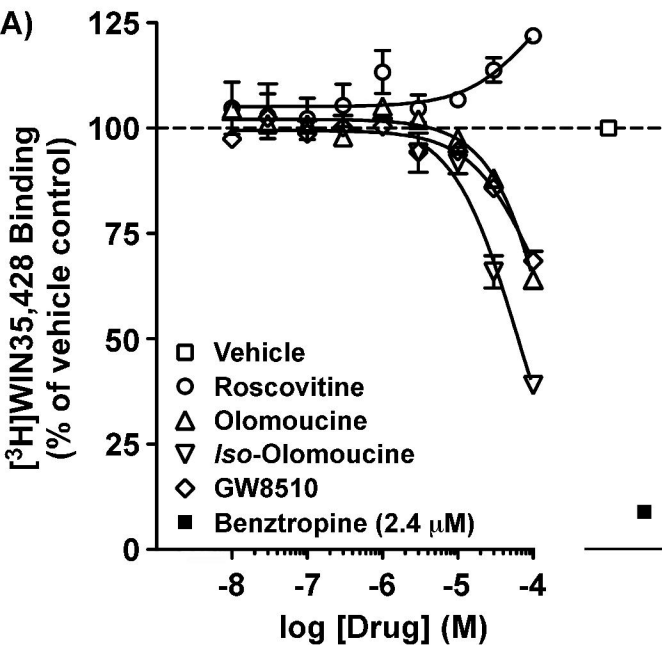


**Figure 3**

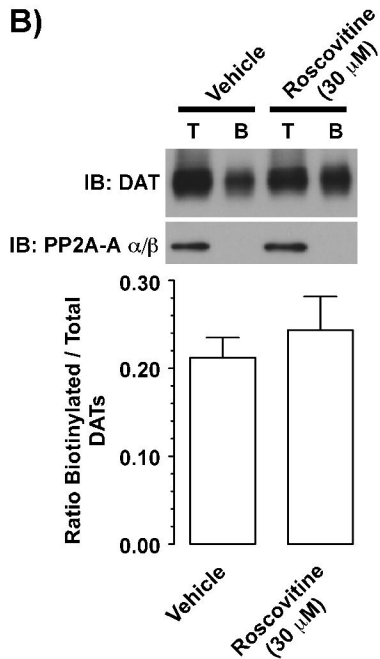
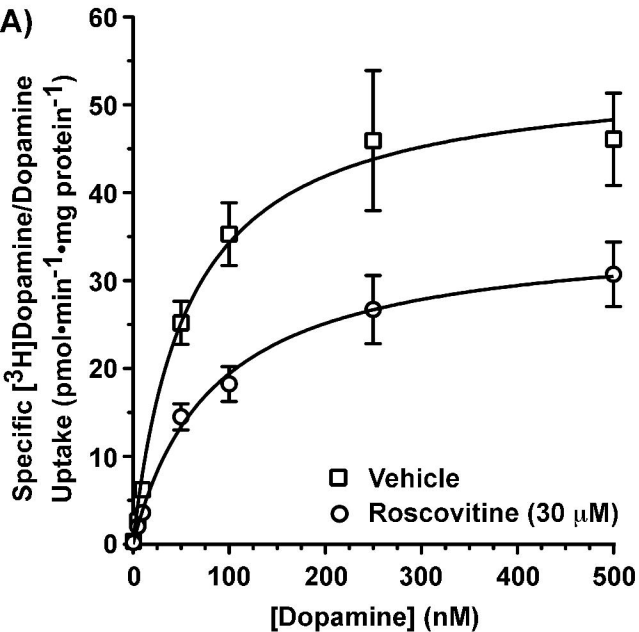


Figure 4

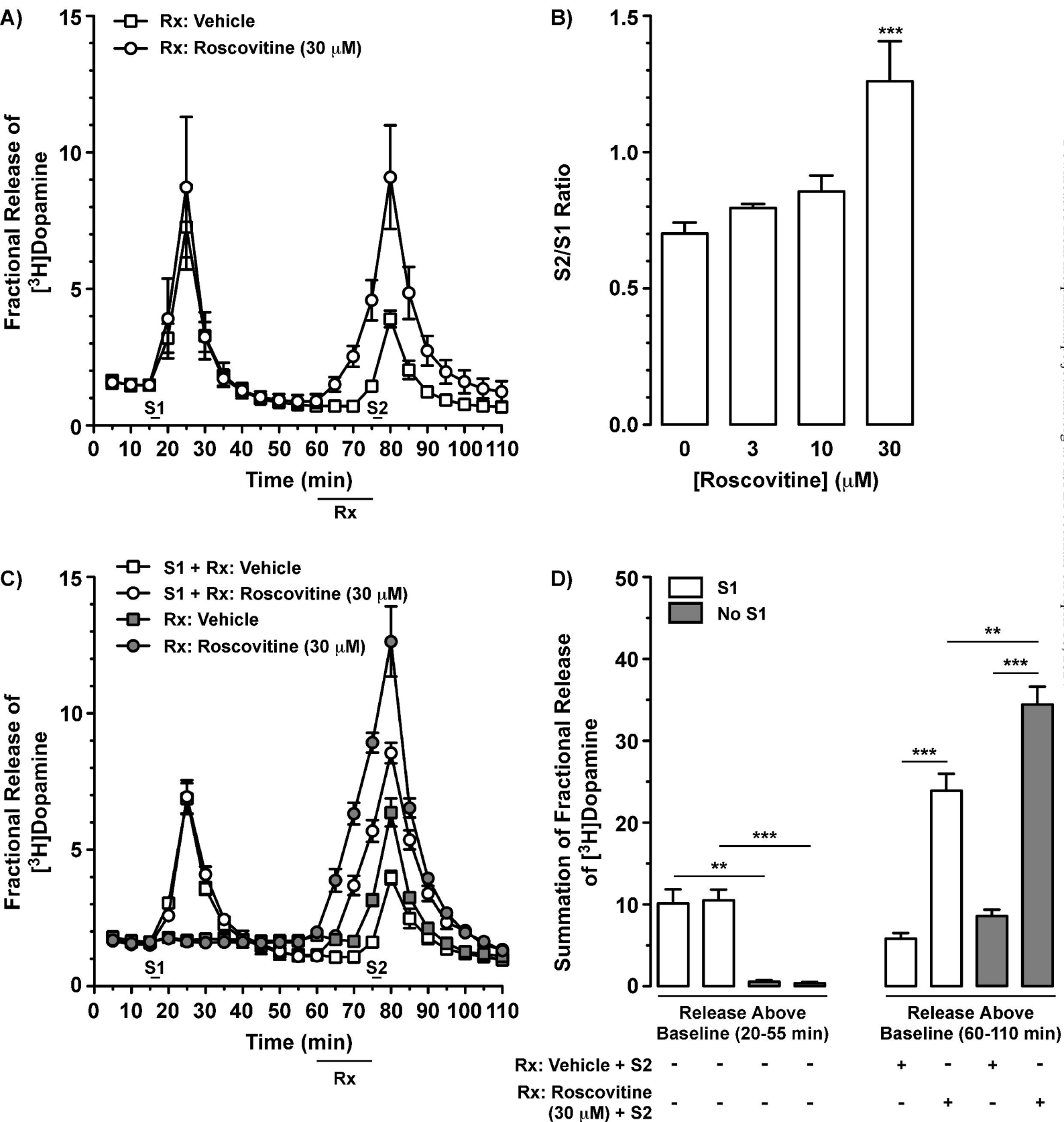


Figure 5

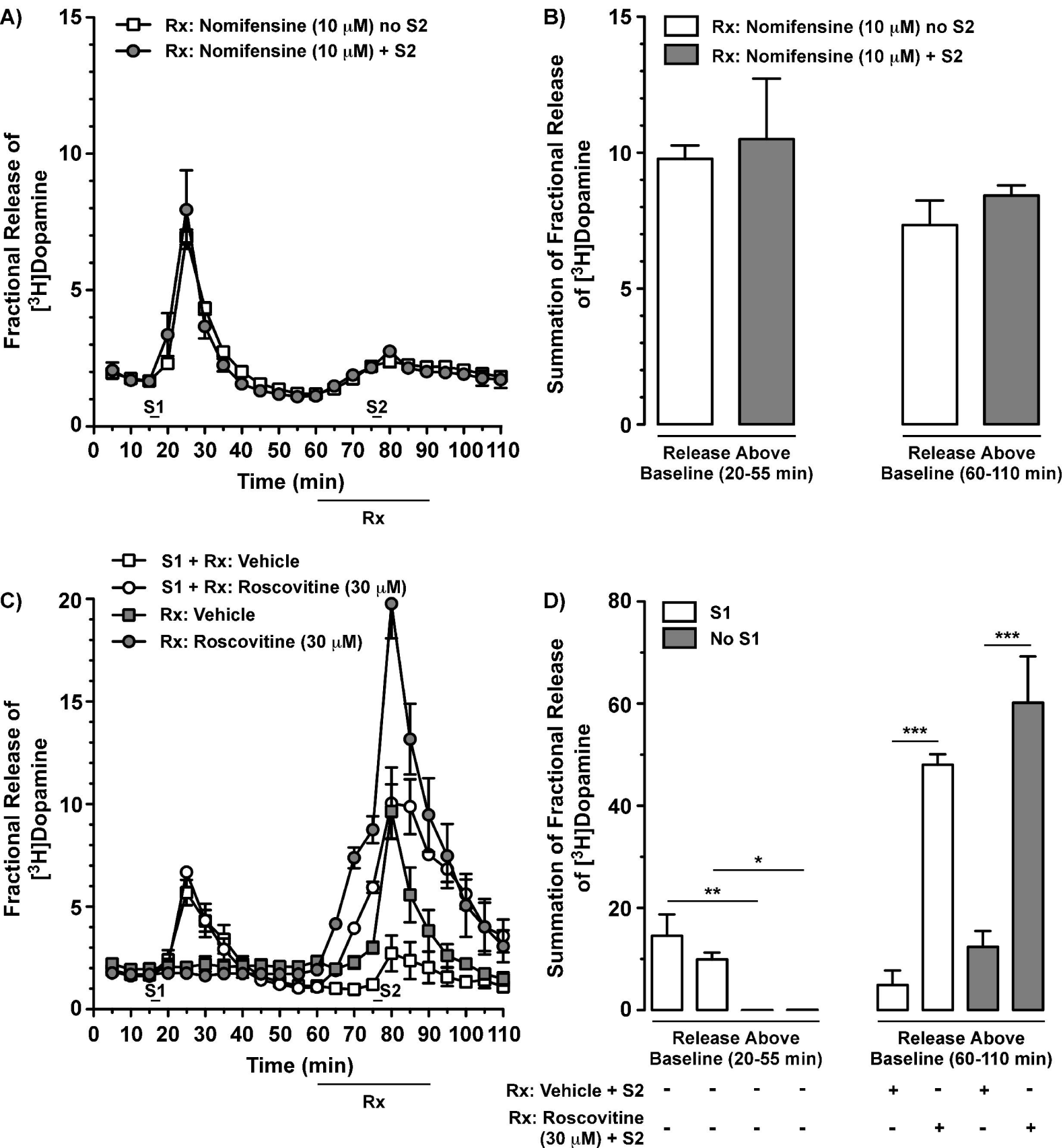
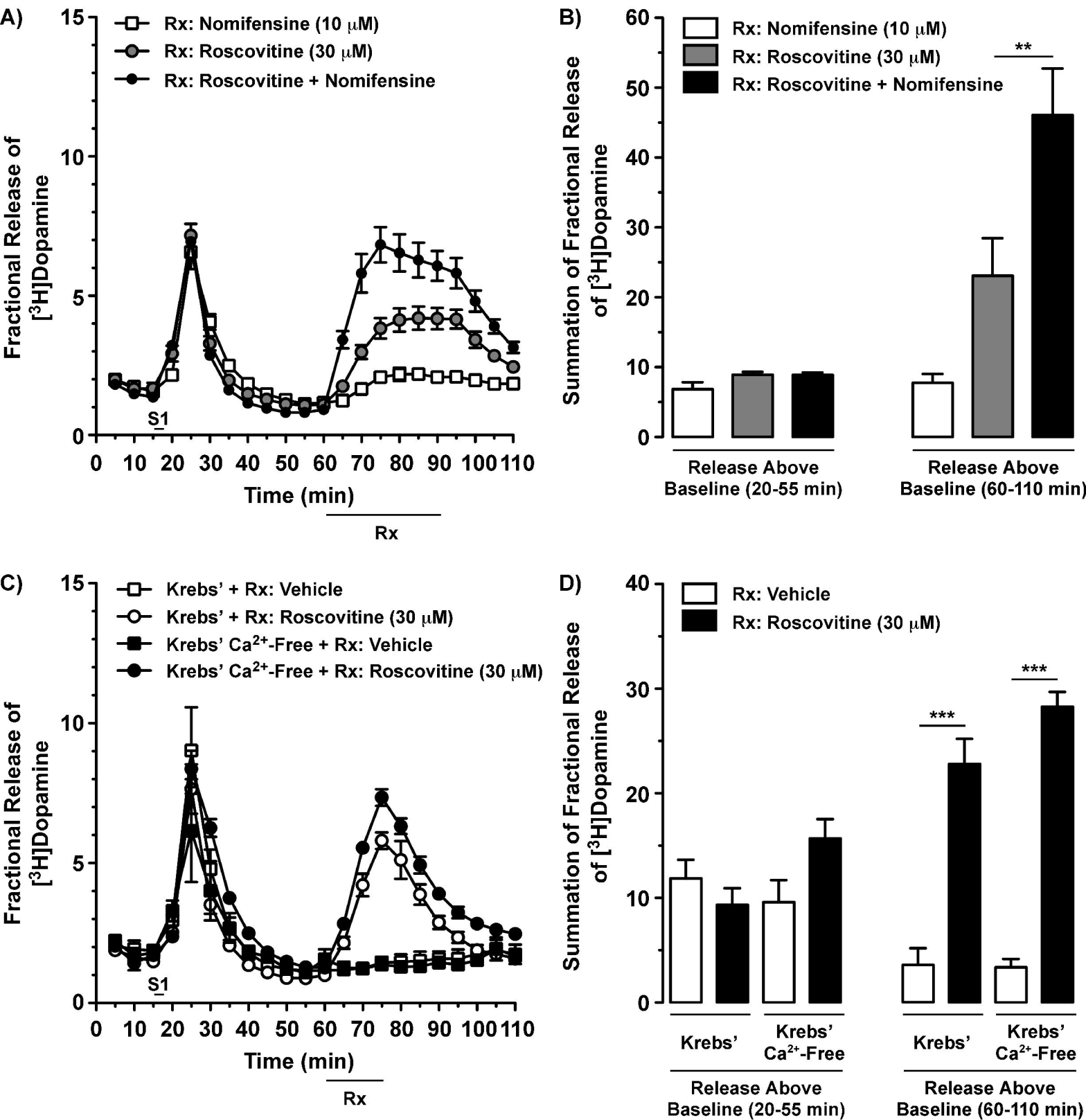
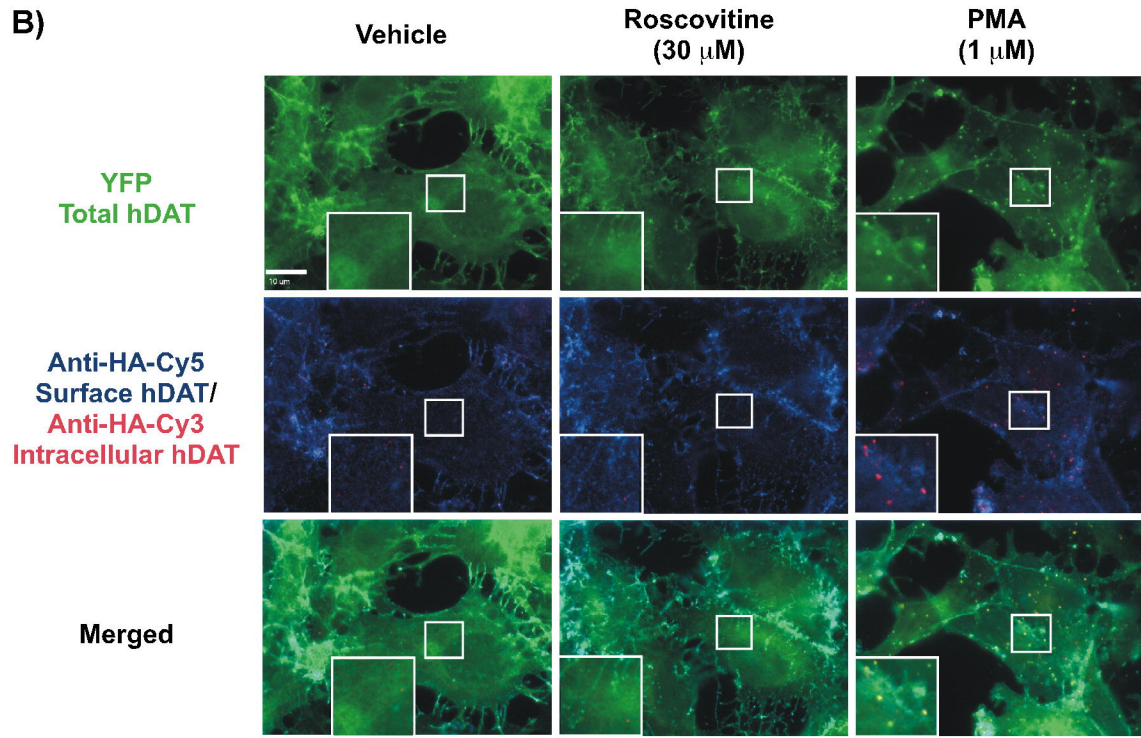
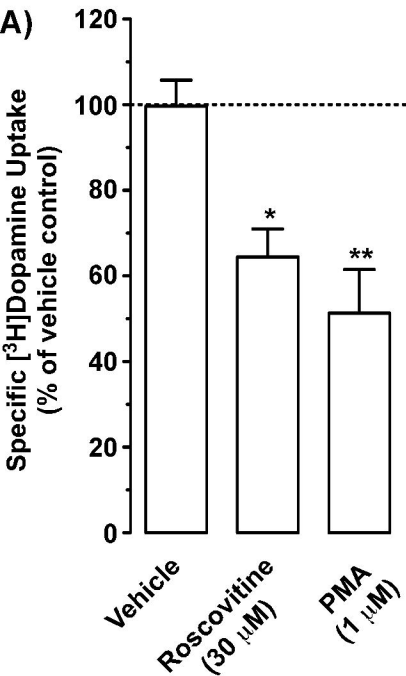
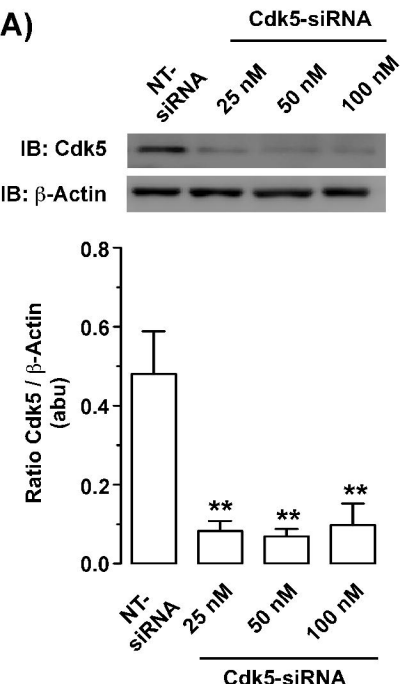


Figure 6



**Figure 7**



**Figure 8****A)****B)**